Electromagnetic Science
vol. 1, no. 2, 0020151, June 2023
https://doi.org/10.23919/emsci.2022.0015

Review

Electric Field Measurement and Application Based on Rydberg Atoms

Bang Liu[1,2], Lihua Zhang[1,2], Zongkai Liu[1,2], Zian Deng[1,2], Dongsheng Ding[1,2], Baosen Shi[1,2], and Guangcan Guo[1,2]

1. *Key Laboratory of Quantum Information, University of Science and Technology of China, Hefei 230026, China*
2. *Synergetic Innovation Center of Quantum Information and Quantum Physics, University of Science and Technology of China, Hefei 230026, China*

Corresponding author: Dongsheng Ding, Email: dds@ustc.edu.cn.
Received December 8, 2022; Accepted February 20, 2023; Published Online June 16, 2023.

Abstract — Microwave sensing offers important applications in areas such as data communication and remote sensing. It has thus received much attention from academia, industry, and governments. Atomic wireless sensing uses the strong response of the large electric dipole moment of a Rydberg atom in response to an external field to achieve precise measurement of a radio frequency (RF) signal. This method offers advantages over traditional wireless sensing including ultrawide energy level transitions, which makes it responsive to RF electric fields over a wide bandwidth. Here, we briefly review the progress of electric field measurement based on Rydberg atoms. We discuss the properties of Rydberg atoms, measurement using Rydberg atoms, experimental progress in electric field measurement of different bands, and different methods for detecting electric fields (such as atomic superheterodyne, machine learning, and critically enhanced measurement). The development of Rydberg atomic measurement focuses on the advantages of Rydberg atomic sensing, especially when compared to conventional microwave receivers. This work is of major significance to developing Rydberg-based measurements in astronomy, remote sensing, and other fields.

Keywords — Rydberg atoms, Microwave sensing, Atomic transition, Machine learning.
Citation — Bang Liu, Lihua Zhang, Zongkai Liu, *et al.*, "Electric Field Measurement and Application Based on Rydberg Atoms," *Electromagnetic Science*, vol. 1, no. 2, article no. 0020151, 2023. doi: 10.23919/emsci.2022.0015.

I. Introduction

Quantum mechanics was established in the early 20th century and became one of the two cornerstones of modern physics. Using quantum technologies, people have greatly improved the ability to manipulate microscopic particles and apply such particles in useful applications. Current applications of quantum technologies include communication, precise measurement, and computing. Quantum precision measurement has been realized in practical applications such as atomic clocks and magnetometers [1] and mainly relies on the accuracy and stability of quantum systems such as atoms and molecules. The applications then uses these systems as standards to measure fundamental physical quantities with high precision. Great progress has been made in atomic-based precision measurements of atomic transition frequencies, which are now used for length and time standards. Atomic clocks have achieved greater precision than 10^{-19} [2]–[5]. Progress has also been made in measuring weak magnetic fields up to a precision of fT/Hz$^{1/2}$ [6]–[9], which promotes applications in encephalopathy and cardiac magnetism measurement. Recently, there has also been increased interest in measuring microwave electric fields [10]–[12] using Rydberg atoms.

A Rydberg atom is a special atom with at least one electron in a highly excited state, which generally requires a principal quantum number $n > 20$. The large electric dipole moment of a Rydberg atom makes it couple strongly to a weak electric field, which can be used to sense electric fields. In response to an applied electric field, the Rydberg atom couples to this external field through its large electric dipole moment and the state of the Rydberg atom changes. Thereupon, the atomic energy levels move, and the relative population of each energy level changes. This change in the atomic state is monitored using electromagnetically induced transparency (EIT) [13], which is an all-optical readout of the Rydberg atomic state [14], [15].

For EIT, probe light can completely pass through the atomic medium within a three-energy-level atomic system interacting with the optical field, which can be explained using quantum optics. Generally, a light beam passing through an atom is absorbed if its frequency resonates with

an atomic energy level, whereas the EIT appears in a three-energy-level system in which the presence of another coupling light causes the probe light to pass completely through the atomic medium (e.g., the atom becomes transparent). In an EIT, a dark atomic state is formed. This special state does not couple to the probe light, which results in EIT capabilities. However, an applied electric field affects the dark state and thus the EIT spectrum of the atom. Thus, for a Rydberg EIT [16], [17], we can use this technique to detect the change of the Rydberg state when the electric field couples with the atom. Then, we obtain the electric field information by detecting the changes of the measured EIT spectrum, including energy level shifts or population changes of the Rydberg atom. Because of the precision of the spectral measurement, the electric field can be measured with high precision.

Compared with traditional antenna measurements, electric field measurements based on Rydberg atoms offer the following advantages through the quantum properties of atoms:

- High sensitivity: Because the large electric dipole moment of a Rydberg atom is extremely sensitive to the external electric field, electric field measurement using the Rydberg atom is a quantum measurement scheme, with a quantum projection limit that far exceeds limits of traditional measurement methods.
- Low noise and immunity to electromagnetic interference: Traditional electric field measurements are based on antennas, which are inevitably affected by thermal noise. For measurements using Rydberg atoms, the atoms packed in glass vapor cells contain no electronic components and thus are immune to thermal noise.
- Large bandwidth: Because of the abundance of energy levels in Rydberg atoms, it is easy to tune these energy levels to couple with electromagnetic waves in a wide range of frequencies from DC to the terahertz (THz) band. This tunability enables sensing and measurement of electric fields in these frequency bands without changing the experimental setup.
- Traceability: For measurement using Rydberg atoms, the optical response properties are traceable to numerous fundamental physical constants. This signifies that the electric fields measured with Rydberg atoms do not require calibration and can be measured directly.
- Portability and integration: The core component for sensing the electric field using Rydberg atoms is a vapor glass cell, which can be on the order of cm in size and is easily carried, integrated, and miniaturized.

Electric field measurements have important applications. In particular, an electric field in the microwave band has strong penetration capability and a long propagation distance while being able to carry a large amount of information. This gives microwave measurement technology great potential in a wide range of applications and widespread research attention. For example, microwave technologies play a very important role in data communication and remote sensing, such as in 5G communication and radar detection. Therefore, electric field measurements based on Rydberg atoms can be used to establish atom-based electric field measurement standards and enable new practical applications.

Here, we introduce the basic principles and applications of electric field measurements based on the Rydberg atom and is organized as follows. Section II introduces the properties of the Rydberg atom and the basic concepts and principles of EIT and the Autler Townes (AT) effect in electric field measurements. Section III presents the basic schemes and principles of using the Rydberg atom to measure electric fields in the frequency range from DC to the THz region. Section IV focuses on applications based on Rydberg atomic measurements of electric fields, especially sensing and communication. Finally, an outlook is presented on Rydberg atomic measurements of electric fields and their applications.

II. Rydberg Atomic Properties

1. Rydberg atom

The Rydberg state is a highly excited electronic state formed by the transition of the outermost electrons of an atom or molecule to an orbital with a higher principal quantum number n [18]. An atom in the Rydberg state is called a Rydberg atom. Because the outermost electron in the Rydberg atom is far from the nucleus, the atom can be regarded as hydrogen-like.

The physical properties of Rydberg atoms can be expressed using formulas similar to those of hydrogen atoms. However, Rydberg atoms have the following special properties, as shown in Table 1.

1) Large atomic radius. According to Bohr's model of the hydrogen atom, the orbital radius of the electron is $r \propto n^2$, where n is the principal quantum number. The principal quantum number of the outermost electron of the Rydberg atom is usually large, so the radius of the Rydberg atom is large.

2) Easily ionizable. The ionization energy of an alkali metal atom is expressed as $E_{nLJ} = -hcR^*/(n^*)^2 = -hcR^*/(n-\delta_{nLJ})^2$, where R^* is the modified Rydberg constant and n^* is the effective principal quantum number, which can be expressed as $n^* = n - \delta_{nLJ}$ (δ_{nLJ} represents the quantum defect for the different quantum numbers n, L, and J). The ionization energy of a Rydberg atom is low for a large principal quantum number n.

3) Small energy spacing. The energy difference between two energy levels is $\Delta E \propto 1/n^2 - 1/(n+1)^2 \approx 2/n^3$, where the principal quantum numbers are n and $n+1$, respectively. The energy level difference between two adjacent Rydberg states is small because n is generally large.

4) Long lifetime. The lifetime of atoms in lower excited states is generally 10^{-8} s, whereas the lifetime of highly excited Rydberg atoms can reach the order of microseconds or even milliseconds.

Table 1 Properties of Rydberg atoms

Property	n dependence	Na (10 d)
Binding energy	n^{-2}	0.14 eV
Energy spacings	n^{-3}	0.023 eV
Orbital radius	n^2	$147a_0$
Geometric cross section	n^4	$68000a_0^2$
Dipole moment ($\langle nd\|er\|nf\rangle$)	n^2	$143ea_0$
Polarizability	n^7	0.21 MHz·cm^2/V^2
Radiative lifetime	n^3	1.0 μs
Fine-structure interval	n^{-3}	−92 MHz

As mentioned above, the Rydberg atom has a large radius, high energy, small energy level difference, and long lifetime. The electric dipole moment of the atom is also large due to its relatively large radius, which makes the Rydberg atom very sensitive to external electric fields. Moreover, the small neighboring energy level difference in the Rydberg atom corresponds to the microwave band. Because of the richness of Rydberg atomic energy levels, changing the principal quantum number n covers a very wide frequency range from low frequency to the THz order, which confers great advantages in electric field measurements.

2. Detection mechanism

EIT is a coherent optical nonlinear phenomenon that was first discovered experimentally by Harris *et al.* [19]. This makes the medium transparent in a narrow spectral range around the absorption line. Rydberg-EIT is a real-time nondestructive method that can directly detect the population of Rydberg atoms. In this subsection, we introduce the mechanism of measurement through the Rydberg-EIT method [11], [12].

The emergence of Rydberg-EIT originates from the dark states that make it impossible for atoms to absorb the probe light. Examining the Hamiltonian eigenstates of the three-level EIT system, the energy of an eigenstate is 0. This eigenstate wave function can be expressed as

$$|D\rangle \propto -|1\rangle + |3\rangle \tag{1}$$

where $|1\rangle$ and $|3\rangle$ are the ground state and Rydberg state, respectively. The eigenstate $|D\rangle$ is called the dark state because its intermediate excited state has zero population. The excited state having zero population signifies no atoms absorb the probe photons through the excited state, i.e., the probe light then passes directly through the atomic vapor without absorption. The dark state is therefore the direct cause of the Rydberg-EIT effect. Thus, we there is a transmission window near the central frequency of the probe light, as shown in Figure 1(a), which corresponds to the dark state.

A microwave field can couple the transition between the uppermost energy level and the fourth energy level, as shown in Figure 1(a). This action splits the transmission spectrum of the probe light, and two transmission peaks appear. When the Rabi frequency of the signal microwave field is much higher than the Rabi frequencies of the probe light and the coupled light, the Rabi frequencies of the probe light and coupled light can be neglected. A pair of microwave-decorated dark states is thus generated with an eigenenergy difference of

$$\Delta E = \hbar\Omega \tag{2}$$

where $\Omega = \sqrt{\Omega_s^2 + \Delta^2}$ is the effective Rabi frequency, Δ is the detuning of microwave, Ω_s is the Rabi frequency of the signal microwave field, and $\hbar$ is Planck's constant. The transmission spectral line is split by the Autler Townes (AT) effect. The splitting interval Δf of the microwave-decorated dark state can be obtained from spectral measurements. Therefore, the electric field strength of the signal microwave field can be inferred from it. In the case of detuning, the relationship between the splitting interval and the Rabi frequency of the microwave field is

$$\Delta f = k\Omega = k\sqrt{\Omega_s^2 + \Delta^2} \tag{3}$$

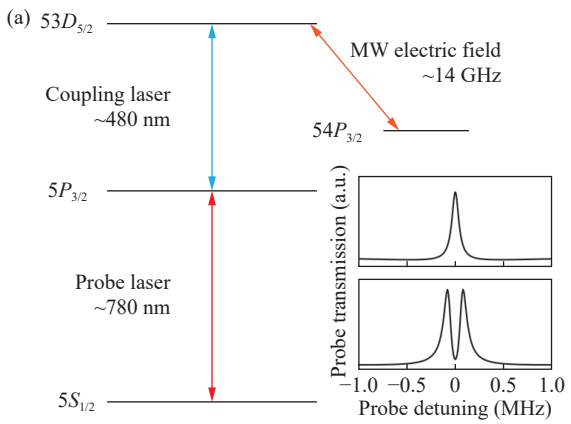

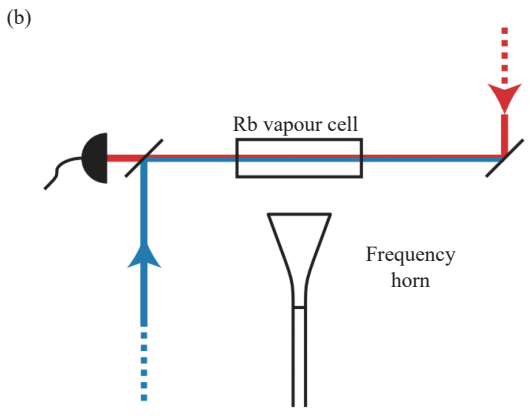

Figure 1 (a) Diagram of a four-level system used to sense the microwave electric field. The top of the illustration shows an example of electromagnetically induced transparency (EIT) associated with a three-level system without a microwave electric field. The bottom of the illustration shows an example of a bright resonance generated within the EIT window when a microwave electric field is present (a.u.: arbitrary units); (b) Experimental apparatus [12].

where k is the correction factor introduced to account for the Doppler effect in the hot atomic system and is 1 for scanning coupling light and λ_p/λ_c for scanning probe light. We obtain

$$E = \frac{\hbar \Delta f}{\mu_r} \tag{4}$$

where μ_r is the corresponding dipole moment. This represents the basic principle of measuring the microwave electric field using the AT splitting of the Rydberg-EIT spectrum.

3. Stark shift

In this subsection, we introduce the interaction mechanism between atoms and an applied electric field, which forms the fundamental principle for sensing electric fields with atoms. In traditional measurement, an external electric field induces a current in the antenna, and then a series of circuits amplifies the signal to measure the electric field. The most significant quantum effect of atoms in an applied electric field is the Stark shift, as was first discovered by Stark in 1913.

Under a DC electric field, an atomic energy level undergoes an energy shift under a DC electric field. When the electric field strength is E, an atom with an intrinsic electric dipole moment undergoes an energy shift $\delta E = \boldsymbol{d} \cdot \boldsymbol{E}$, which is called the linear Stark effect. If the intrinsic electric dipole moment is 0, an electric dipole moment $\boldsymbol{d} = \alpha \boldsymbol{E}$ is induced under the electric field, where α is the polarizability of the atom. The energy level shift is thus $\delta E \propto \alpha E^2$, which is called the squared Stark effect [20], [21].

For an AC electric field, the effect differs based on the electric field frequency. A nonresonant weak electric field shows a similar effect to that of direct current; i.e., energy level shifts occur. A strong field induces sidebands in the spectrum that are explained by Floquet theory [22]–[24]. Resonant electric fields induce AT splitting, as described above.

Thus, atoms show different perturbations under an external electric field that result in different responses in the EIT spectrum. In turn, we record details of the EIT spectrum to obtain information on the electric field.

III. Electric Field Measurement

1. DC electric field measurement

The polarizability of a Rydberg atom is proportional to n^7, and the electric field strength threshold for field ionization is proportional to n^{-4} [18]. Therefore, atoms in the Rydberg state are very sensitive to the electric field, and the magnitude of the weak electrostatic field can be measured by recording the Rydberg atomic level shift through microwave [25]–[27] or laser [28], [29] spectroscopy. The Stark shift of the Rydberg state is measured from the vacuum UV-millimeter double-resonance spectrum of the high Rydberg state of the krypton atom [26]. As discussed in the previous section, the Rydberg atom produces a Stark energy shift $\delta E = \alpha E^2$ in an external DC electric field, such that the magnitude of the applied electrostatic field can be obtained by simply measuring the energy shift through the spectrum. The minimum electrostatic field strength that can be measured is ±20 μV/cm [26].

In this configuration, Rydberg atoms are detected through field ionization, resulting in a destructive detection scheme that does not permit real-time continuous electric field measurement. In addition, this measurement scheme is primarily limited by the resolution of the acquired spectrum; thus, a higher-energy UV laser is required to excite the atoms to higher Rydberg states.

2. Low-frequency electric field measurement (kHz)

A low-frequency electric field on the order of kHz primarily causes a Stark shift when interacting with Rydberg atoms; thus, it is still necessary to measure the Rydberg energy level shift to obtain information on the electric field. However, the atoms are usually held in a glass container, and the atomic species are usually alkaline metals such as Rb and Cs, as shown in Figure 2. These alkali metal atoms are adsorbed on the inner surface of the glass container, causing low-frequency electric field shielding [30], [31]. Only when the electric field oscillates at high frequencies (e.g., from the sub-MHz to the THz order) can it penetrate the glass cell and be detected by the atoms [32]–[35]. Therefore, the electromagnetic shielding effect of glass vapor must be considered when measuring low-frequency electric fields.

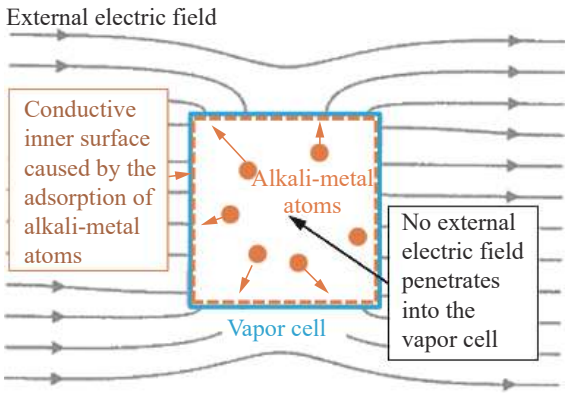

Figure 2 Adsorption of alkali metal atoms causes the inner surface of the vapor cell to be slightly conductive. When a low-frequency external electric field is applied, the free charge on the inner surface is redistributed to maintain an equipotential state, and no electric field enters the vapor cell [36].

For this purpose, prior efforts have used an Rb gas vapor cell made from sapphire single crystals with very slow electric field shielding times, e.g., on the order of seconds [36]. Low-frequency electric fields were measured using a sapphire gas vapor cell with a light-sensing internal bias electric field. This process is sensitive enough to respond linearly to an external electric field. Such a sensor can be used to monitor weak ambient AC electric fields and other

electronic noise and to remotely detect moving charged objects. The main sensitive unit of this atomic sensor exhibits an effective volume of 11 mm^3 and provides a scattering noise limit of approximately 0.34 $mV/(m\cdot Hz^{1/2})$ with a low 3-dB cutoff frequency of approximately 770 Hz [36].

This approach enables additional applications in atomic electric field sensing, such as calibration of DC and low-frequency electric fields, communication in the extremely low-frequency (ELF) and ultralow-frequency (ULF) bands (kHz or below), and activity detection through remote sensing, geoscience, and bioscience.

3. Intermediate-frequency electric field measurement (MHz)

1) Intermediate-frequency strong-field measurement

For an intermediate-frequency (IF) electric field in the MHz band, there is almost no resonance with the Rydberg atomic energy levels; thus, the coupling with the Rydberg atoms is primarily nonresonant. A weak applied MHz field leads to a Stark shift, and the resulting energy level shift is proportional to the square of the electric field amplitude. However, for a strong MHz field, a general perturbation calculation fails due to the relatively strong interaction [37]–[40]. In this case, the Floquet method is used to solve for the response of the atoms to the electric field. The Rydberg level is then modulated by the applied electric field, and a series of discrete energy levels is produced in which the spacing between levels equals the frequency of the applied electric field (in natural units). The energy levels of an atom are

$$\delta_N = E^{(0)} - \frac{\alpha^2}{2}E_{\mathrm{DC}}^2 - \frac{\alpha^2}{4}E_{\mathrm{AC}}^2 + N\hbar\omega_m \tag{5}$$

where $E^{(0)}$ corresponds to the energy of the atomic state, $E_{\mathrm{DC,AC}}$ represents the amplitudes of the DC and AC fields, N is the sideband order, and ω_m is the frequency of the applied electric field. The EIT spectrum exhibits the sideband characteristics shown in Figure 3. The interval between the sidebands and the main peak reflects the electric field frequency, and the signal height reflects the electric field strength. By comparing the calculated and experimental spectra, we obtain the electric field strength with an uncertainty of 3%, corresponding to a minimum measurable electric field of 1 V/cm [29], [41], [42].

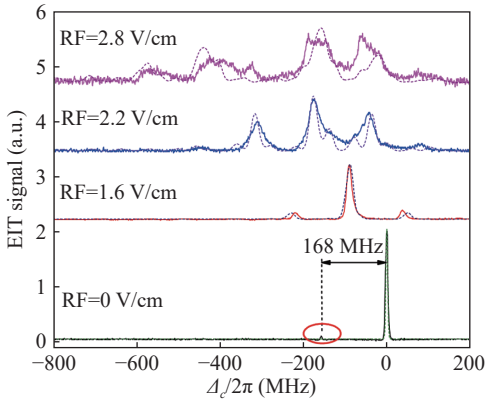

Figure 3 Measured (solid line) and calculated (dashed line) Rydberg EIT spectra under RF modulation (modulation frequency $\omega_m = 2\pi\times 70$ MHz) and the indicated RF field amplitudes [41].

In strong MHz fields, adjacent hydrogen-like manifolds begin to intersect displacement levels, providing a rich spectral structure suitable for precision field measurements. Each energy level position $\omega_{v,N}$ and transition probability $S_{v,N}$ can be calculated as

$$\hbar\omega_{v,N} = W_v + n\hbar\omega_{\mathrm{RF}} \tag{6}$$

$$S_{v,N} = (eF_L/\hbar)^2\left|\sum_k \tilde{C}_{v,k,N}\cdot\langle k|\hat{r}|5P_{3/2},m_J\rangle\right|^2 \tag{7}$$

More details can be found in [42]. An RF electric field is determined by matching observed spectral signatures, including AC level shifts, even harmonic RF sidebands, and RF-induced avoidance crossings in the Rydberg manifold, with the spectra calculated from nonperturbative Floquet theory. The measurement precisions for the RF field frequency and electric field amplitude are 1.0% and 1.5%, respectively, and the maximum field strength reaches 5 kV/m [43], [44].

2) Intermediate-frequency weak-field measurement

The previous subsection described how the interaction between an IF strong field and a Rydberg atom causes modulation sidebands in the EIT spectrum and more complex energy level crossings. These sidebands and the information on the energy level crossing can be used to determine the electric field strength. However, this method is limited to characterizing intermediate to strong electric fields. When a weak IF electric field is applied, the perturbation to the Rydberg atoms is very small, and only a small perturbation is generated in the spectrum. This spectral resolution limit makes it difficult to measure such small disturbances. Therefore, we discuss a measurement scheme using a superheterodyne receiver, where a local oscillator field is introduced to amplify the system response to the weak IF electric field and measure the field. At an electric field frequency of 30 MHz, a minimum field strength of 30 μV/cm is obtained with a sensitivity of up to −65 dBm/Hz and a linear dynamic range of over 65 dB [45].

The long wavelength and long propagation distance of a MHz RF electric field make it very significant in fields such as shortwave international and regional broadcasting and aviation air-to-ground communication. The main advantage of using Rydberg atoms to measure an IF electric field is that the volume of the sensing unit can be made very small, reaching the order of cm. Meanwhile, Rydberg atom-based electric field sensors enable measurements from weak fields on the order of A/cm to strong fields on the order of kV/m. Because of these advantages, electric field sensors based on Rydberg atoms are expected to be used in more applications, such as long-distance communication, over-the-horizon radar, and RF identification (RFID).

4. High frequency electric field measurement (GHz)

For a microwave electric field with a frequency exceeding 1 GHz, resonant interactions with the Rydberg atom occur because the frequency is close to the adjacent energy levels of the Rydberg atom, resulting in AT splitting in the EIT spectrum. This effect can be used to measure electric fields, as we describe in detail below.

1) Measurement of a microwave electric field through AT splitting

AT splitting of a Rydberg atom was first used to measure a microwave electric field by Sedlacek, *et al.* in 2012 [12]. A sensitivity of 30 μV/(cm·Hz$^{1/2}$) was obtained, and the minimum detectable field was as low as 8 μV/cm. The electric field detection is shown in Figure 1.

Subsequent improvements have been made using active control of frequency-modulated spectroscopy and residual amplitude modulation (AM) to improve signal-to-noise ratio of the optical readout of Rydberg atom-based RF electrometry [46]–[48]. A sensitivity up to 3 μV/(cm·Hz$^{1/2}$) can be achieved, reaching the photon shot noise limit [49].

2) Atomic superheterodyne measurement

Using the AT splitting of the spectrum to measure the electric field has certain limitations. This occurs because the derivation requires the Rabi frequency of the microwave electric field to be sufficiently strong i.e., the electric field strength is relatively strong and AT splitting is only suitable for measuring intermediate and strong fields. Because a weak field is insufficient to split the spectrum, it only reduces the EIT peak. Therefore, new methods are needed to measure a weak field. Next, we describe how introducing a local oscillator electric field into a superheterodyne system greatly improves the sensitivity of measuring electric fields.

The Rydberg-superheterodyne process is as follows. The local oscillator (LO) signal E_L of a strong near-resonant microwave produces AT splitting in its spectrum. This signal and the signal to be measured, E_S, pass through the Rydberg atom. The interaction mixes frequencies, as shown in Figure 4, and the resulting IF signal P_0 is loaded onto the EIT spectrum.

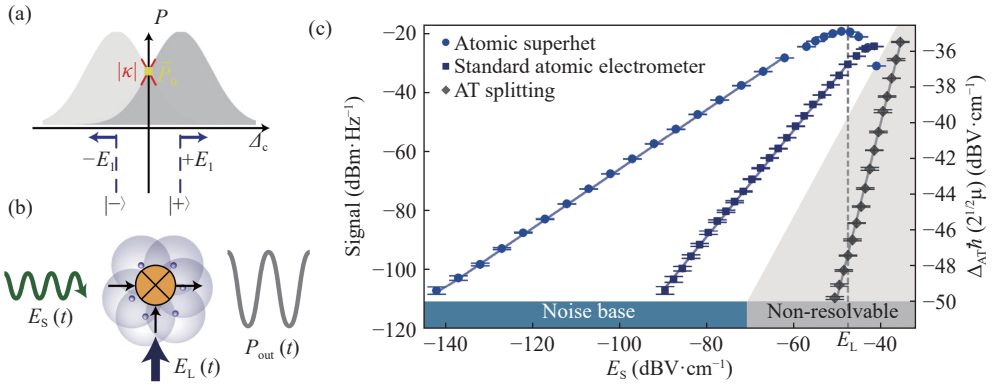

Figure 4 (a) and (b) Schematics of the principles of a superheterodyne Rydberg atomic receiver, where E_s is the amplitude of the signal microwave field to be measured, E_L is the amplitude of the local oscillating microwave field, and the output signal P_{out} is read out through EIT spectroscopy. (c) Comparison of the sensitivities of atomic electric field meters and atomic superheterodyne measurement systems [11].

The strong local oscillator microwave field causes the atom to produce two $\hbar\Omega_L$ dressed states with an energy interval of $|\pm\rangle$, where Ω_L is the Rabi frequency of the local oscillator field. When the very weak signal field is loaded on the atom, the energy shift $|\pm\rangle$ of the two dressed states is

$$\pm E_1 = \pm\hbar\Omega_s\cos(2\pi\delta_s + \phi_s)/2 \tag{8}$$

where Ω_s is the Rabi frequency of the signal field, δ_s is the amount of frequency detuning of the signal field relative to the local oscillator field, and ϕ_s is the phase difference between the signal and the local oscillator. The energy shift of these two dressed states results in a linear change in transmittance at the center of the EIT spectrum (at resonance). This relationship between the transmittance change $P_{out}(t)$ and the signal electric field is

$$P_{out}(t) = |P(\delta_s)|\cos(2\pi\delta_s t + \phi_s) \tag{9}$$

Here, $P_{out}(t) = P(t) - \overline{P}_0$ is the change in transmittance relative to the transmittance $\overline{P}_0$ under a no-signal electric field, and $|P(\delta_s)|$ is the single-sided Fourier spectrum corresponding to a frequency of δ_s. The transmittance change is proportional to the Rabi frequency of the signal field and described as follows

$$\Omega_s = |P(\delta_s)|/|\kappa_0| \tag{10}$$

The intensity of the signal microwave electric field is measured by measuring the intensity of the beat frequency. This scheme has been successfully demonstrated experimentally at Shanxi University [11] with a sensitivity reaching 55 nV/(cm·Hz$^{1/2}$). This minimum detectable field is three orders of magnitude lower than what can be achieved with AT splitting. This Rydberg atomic superheterodyne receiver allows traceable International System of units (SI) measurements with an uncertainty of 10^{-8} V/cm and allows phase and frequency detection. Such an approach makes it possible to measure microwave electric fields using Ryd-

berg atoms with much higher sensitivity, greatly enhancing the use of Rydberg atoms to measure weak electric fields.

3) Enhanced precision via the critical point of the phase transition in Rydberg atoms

Because of the large interaction volume and the strong many-body interactions in the system, Rydberg atoms near the phase transition point produce an avalanche transition in response to a very small disturbance. In other words, the atoms in the many-body Rydberg state excite surrounding atoms to many-body Rydberg states, thus amplifying the effect of small perturbations on the Rydberg atoms. This property can be used to further enhance the precision and sensitivity of Rydberg atoms to detect microwave electric fields by detecting the steep optical spectral of Rydberg atoms to microwaves near the phase transition point [50]–[52].

There exists a discontinuous phase transition in Rydberg atoms that is characterized by a sharp edge in the transmission spectrum [53], [54]. This phase transition is caused by the avalanche generated by the interaction between Rydberg atoms, which makes the number of Rydberg atoms change significantly at the critical point of the phase transition. This critical phenomenon was recently used to sense a microwave electric field [55]. If an external microwave electric field is applied at this time, then the spectral lines move because of the Stark effect as shown in Figure 5(b). The shift of the steep edge is more distinct than the overall movement; i.e., the change in the external field is more significant at the edge. Compared with using the overall spectral shift, using the critical point of the phase transition to measure the microwave electric field is equivalent to using a ruler with a finer scale, so the field can be measured with higher precision.

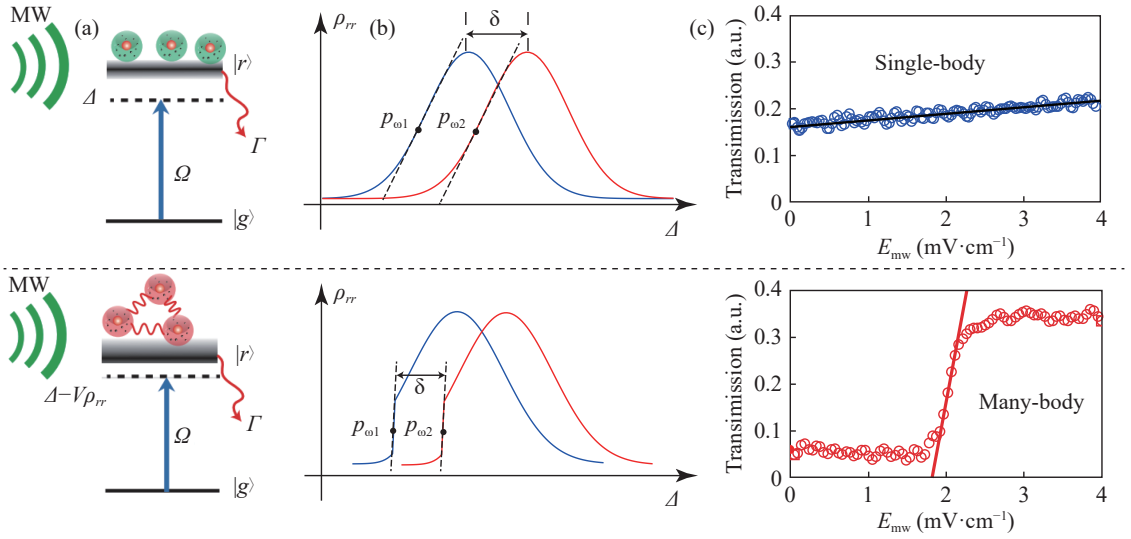

Figure 5 Principles of single-body (top row) and many-body (bottom row) Rydberg metrology. (a) Energy diagram for a two-level atom showing the ground state $|g\rangle$ and Rydberg state $|r\rangle$. In the many-body case, the Rydberg resonance is modified by the many-body interaction strength, $V = C_6/r^6$. (b) The blue and red curves represent the spectra with and without an external microwave field, respectively, which induce a shift δ. The measurement sensitivity is highest when the derivative $d\rho_{rr}/d\Delta$ is maximal, as indicated by points p_{w1} and p_{w2}. The steeper slope near the critical point in the many-body case (bottom row) results in enhanced measurement sensitivity. (c) Transmission occurs under different microwave field amplitudes for the single-body and many-body cases. The steep edge at E_{mw} =2.0 mV/cm indicates that the tiny variance of the microwave field induces a giant change in the transmission, and thus, the sensitivity of the many-body case is higher than that of the single-body case [55].

4) Microwave-to-optics conversion through Rydberg atoms

Nonlinear optical processes such as four-wave and six-wave mixing can be realized using the atomic energy level structure. Microwave photons in these nonlinear optical processes can be converted to optical bands by choosing suitable energy levels [56]–[59]. Researchers at South China Normal University have realized six-wave mixing using a cold atomic system to efficiently convert microwave photons to optical bands through microwave coupling of the transition of two neighboring Rydberg energy levels [60]. That experiment was based on a two-dimensional cold atomic system with a large optical depth, and the conversion efficiency reached 82% with a bandwidth close to 1 MHz. This reliably converted single-photon quantum states from the microwave domain to the optical domain, and the relevant mechanism was used to convert dozens of microwave photons to the optical band. A practical example of such an effect is using single-photon counters to measure the photons after microwave conversion. The maturity of this technology enables precise measurement of microwaves with a sensitivity on the order of tens of microwave photons, which can be used for detection and imaging of weak microwave photons.

5. Terahertz electric field measurement

The terahertz band is suitable for nondestructive testing because of its ability to penetrate materials such as papers,

plastics, and clothes [61], [62]. Detectors in the THz region are typically less sensitive than those in other regions of the EM spectrum. Researchers at Durham University have demonstrated a THz imaging system based on THz-to-optical conversion in a room-temperature atomic vapor [63]. This system allowed image acquisition with high speed and sensitivity. Furthermore, many adjustments remain feasible to improve its future performance.

Electric dipole transitions between neighboring Rydberg states of alkali atoms lie in the THz range[18], [64]. THz-to-optical conversion is achieved based on laser-excited Cs Rydberg states ($13D_{5/2}$) emitting a photon at 535 nm when the Rydberg atoms absorb a THz photon, in which the conversion efficiency is approximately 52.4%. Then, when a 2D sheet of atoms is created, these emitted photons display a full-field image of the incident THz field in a single exposure. In one experiment [63], the system was used to capture the free fall of a water droplet, and the THz imaging of the dynamic process in the frame rose to 3 kHz. That work showed that the system achieves resolution near the diffraction limit and is capable of high-speed imaging.

IV. Application

A Rydberg atom is therefore very promising in applications due to its advantages in electric field measurement [65]–[68], including its extremely wide detection frequency range and high sensitivity. Researchers have applied great effort to expanding its applications [69], as discussed in the following.

1. Communication

Microwave electric fields are widely used in communication because of their large channel capacity, fast transmission rate, and long transmission distance. 5G communication is one example of an application operating in the microwave band. Rydberg atoms can be used to receive such signals because they respond to microwave radiation [70], [71].

1) Analog communication

Atom-based microwave communication is accessible through the microwave electric field measurement introduced above [72]. To realize microwave communication, the baseband information must be modulated to the microwave, and then the Rydberg atom serves as a microwave receiver that demodulates the baseband signal.

The carrier electric field E_c is written as

$$E_c = E_0\cos(\omega_0 t) \tag{11}$$

The modulated electric field E_s is

$$E_s = E_1\cos(\omega_1 t) \tag{12}$$

Then, the modulated carrier electric field is expressed as

$$E(t) = E_0\left(1+\frac{E_1}{E_0}\cos(\omega_1 t)\right)\cdot\cos(\omega_0 t) \tag{13}$$

where ω_0 is the carrier frequency and ω_1 is the modulation frequency. The modulated carrier amplitude is written as

$$|E(t)| \approx E_0 + E_1\cos(\omega_1 t) \tag{14}$$

In the EIT readout scheme, the transmittance of the probe light is

$$T_{\text{probe}} \propto |E(t)| \approx E_0 + E_1\cos(\omega_1 t) \tag{15}$$

We observe that when the EIT scheme is used as a readout, the Rydberg atom has the ability to remove the carrier wave. The high-frequency carrier resonates with the Rydberg atomic energy level, and its frequency components are eliminated. The result is that only the low-frequency modulation signal remains in the spectral signal. Therefore, one advantage of using Rydberg atoms for microwave communication is to obviate the need for a complex demodulation device because the Rydberg atom itself can complete the demodulation. The atom filters out the carrier wave and directly demodulates the baseband signal in the probe light signal. To restore the baseband signal, one needs to measure the intensity change of the probe light.

Using the above principles, Georg Raithel, *et al.* experimentally demonstrated amplitude modulation (AM) and frequency modulation (FM) communication using Rydberg atoms [73], [74], which received, replayed, and recorded baseband signals in the audio range, as shown in Figure 6. They used the audio signal to modulate the amplitude or frequency of the microwave carrier wave. The modulated microwaves were detected by the atoms, and the microwaves were demodulated through direct real-time detection of the atomic EIT spectra. Experiments have shown that multiband AM and FM communication are possible using the rich energy levels of Rydberg atoms. The atomic radio receiver eliminated the need for conventional demodulation and signal-conditioning circuits, making the atomic radio inherently resistant to electromagnetic interference. In addition, the 3-dB bandwidth for communication using this atomic radio receiver was approximately 100 kHz and limited by the EIT linewidth, transit time, and other factors [75]. The instantaneous bandwidth of the atomic receiver was only a few hundred kHz, which was shorter than that in conventional communications. Therefore, this design is certainly more than sufficient for transmitting sound signals but cannot satisfy efficiently transmitting information at higher frequencies.

Holloway *et al.* used Rydberg atoms in the real-time recording of musical instruments [76]. In addition, they recorded two guitars simultaneously using two different atomic elements (Cs and Rb) in the same vapor cell. Each atomic element can be detected, and each Rydberg atom-based guitar could be recorded separately.

2) Digital communications

Rydberg atoms can also be used to measure the phase of the microwave electric field through the phase modulation of

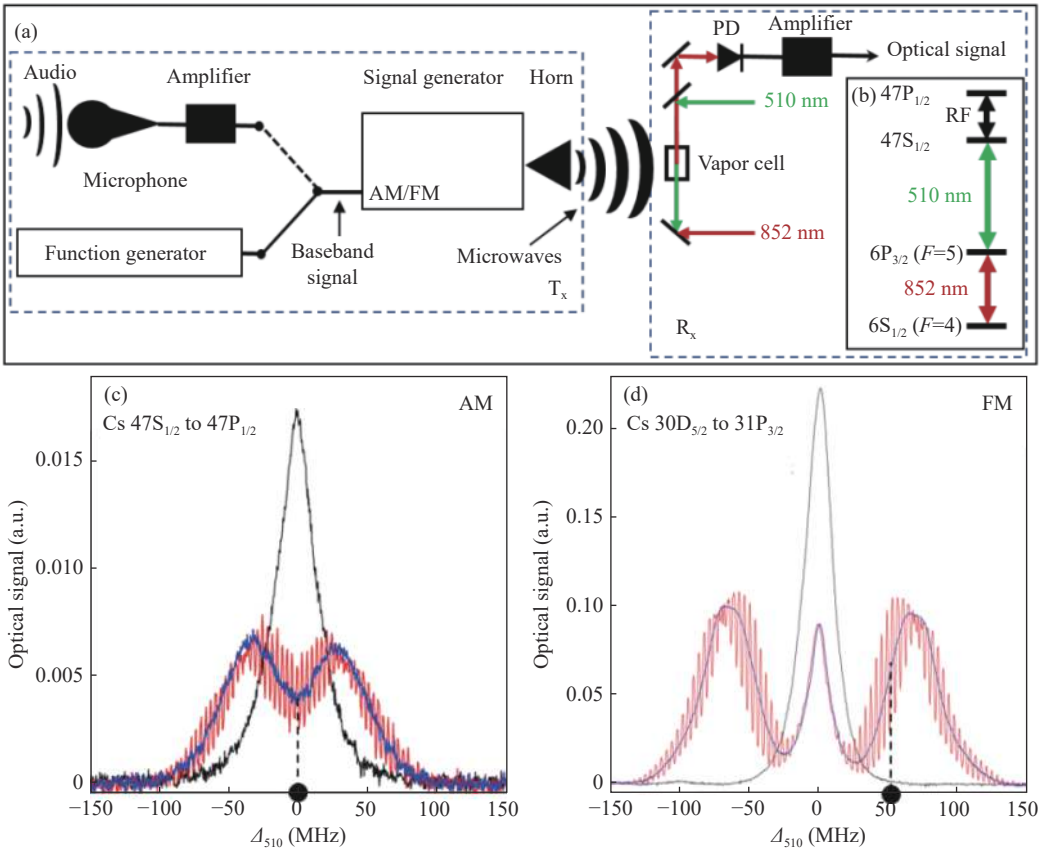

Figure 6 (a) Experimental setup. (b) Energy level diagram. (c) EIT spectrum under amplitude modulation (AM) (red), with the carrier amplitude modulated at a baseband AM frequency of 1 kHz and modulation depth of ±25% . (d) EIT spectrum under frequency modulation (FM) (red), with the carrier frequency modulated at a baseband FM frequency of 1 kHz and modulation deviation of ±30 MHz [73].

the field, after which the Rydberg atoms can be used to measure the microwave electric field to achieve digital communication [77]. Paul, *et al.* demonstrated that room temperature Rydberg atoms can be used as sensitive, high-bandwidth microwave communication antennas [78]. Using an EIT detection scheme, they read out data encoded in AM 17-GHz microwaves near the photon shot noise limit. The channel capacity was up to 8.2 Mbit/s, and an 8-state phase-shift keying (PSK) digital communication protocol was implemented, as shown in Figure 7.

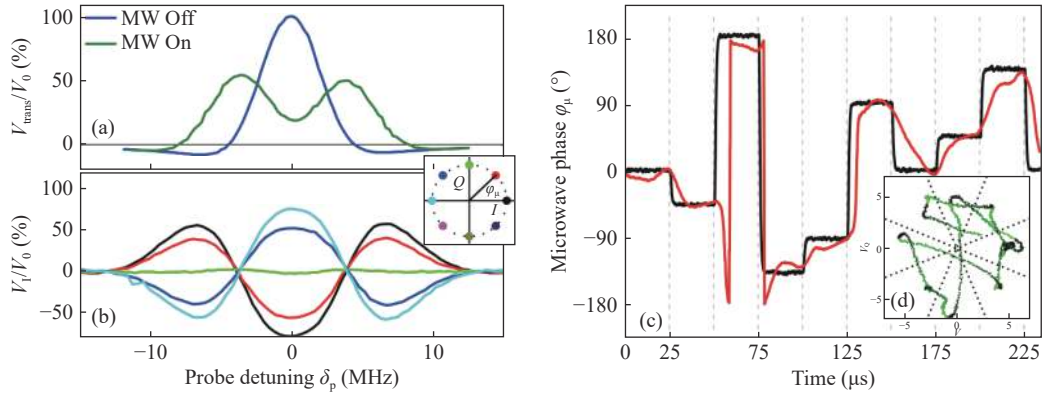

Figure 7 (a) Rydberg EIT (blue) and Rydberg EIT-AT splitting (green). (b) Examples of demodulated transmission signals with each color corresponding to a different AM phase. (c) PSK sent and received phases (black and red, respectively). (d) Phase constellation of the received phase in (c) (red line); more details are in [78].

For digital microwave communication based on the Rydberg atomic system, Paul *et al.* also studied the standard quantum limit of theoretical data capacity and experimentally observed quantum-limited data reception with bandwidths from 10 kHz to 30 MHz. This work provided an alternative to microwave communication, which relied

on conventional antennas. The efficiency of traditional communication antennas was significantly reduced, especially when the antenna was significantly smaller than the electromagnetic field wavelength. However, the efficiency of the Rydberg atomic system was not affected by antenna size [79].

Others have studied the feasibility of digital communication with nonresonant and continuously tunable RF carriers through Rydberg atomic receivers [80]. Their experiment showed that digital communication at a rate of 500 kbps can be reliably achieved within a tunable bandwidth of 200 MHz near a 10.22-GHz carrier wave. This experiment solidified the physical foundation for reliable communication and spectral sensing with wider-broadband RF carriers, paving the way for concurrent multichannel communication based on the same pair of Rydberg states.

3) Deep-learning-enhanced Rydberg atomic multifrequency microwave recognition and communication

Practically, it is challenging to identify multifrequency microwave electric fields due to the complex interference between such fields. The excellent properties of Rydberg atoms make them broadly applicable to multifrequency measurements in microwave radar and microwave communications. However, Rydberg atoms they are sensitive not only to microwave signals but also to noise from atomic collisions and the environment, which results in the solution of the Lindblad master equation for light-atom interactions being complicated by noise and higher-order terms. A group of University of Science and Technology of China (USTC) solved these problems by evaluating Rydberg atoms with a deep learning model, demonstrating that deep learning leverages the sensitivity of Rydberg atoms and reduces the effects of noise without solving the master equation [81]. This receiver directly decoded frequency division multiplexed (FDM) signals without multiple bandpass filters and other complex circuits, as shown in Figure 8. In this proof-of-principle experiment, an FDM phase-shift keying signal carrying a noisy QR code was effectively decoded with an information transmission rate of 6 kbps for four bins and an accuracy of 99.32%. This new technology is expected to benefit Rydberg-based microwave field sensing and communication.

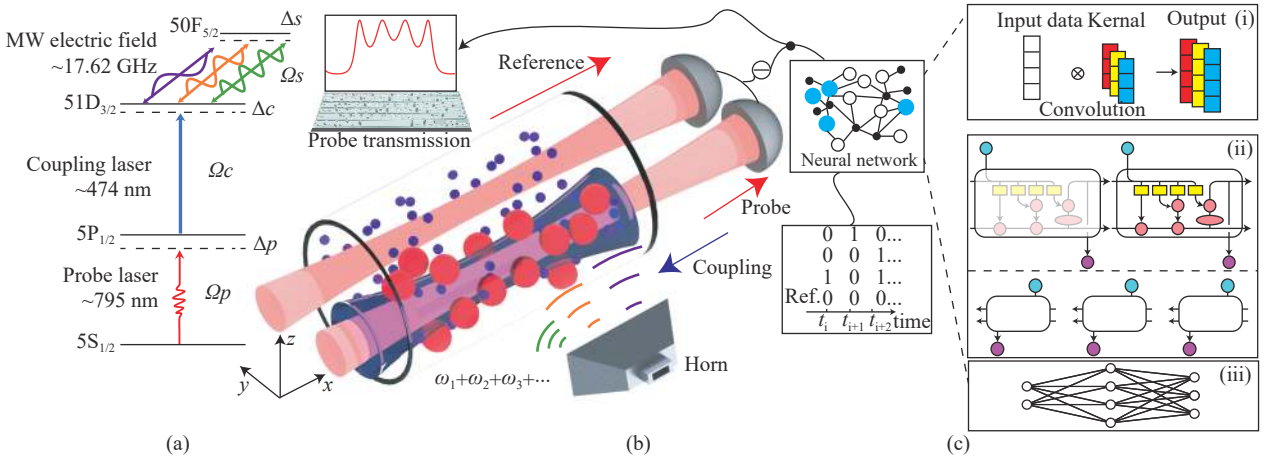

Figure 8 Illustration of the setup. (a) Experimental energy diagram. (b) Schematic of a Rydberg atom-based antenna and mixer interacting with multifrequency signals. The probe light and the counterpropagating coupling light form the EIT configuration. Multifrequency microwave fields transmitted by a horn are applied to the atoms, with a radiating direction that is perpendicular to the laser beam propagation direction. The multifrequency microwave fields are modulated using a phase signal carrying the messages. The probe transmission spectrum is fed into a well-trained neural network to retrieve the variations in the phases with time. (c) Schematics of the neural network. The network consists of (i) a one-dimensional convolution layer, (ii) a bidirectional long-short term memory layer, and (iii) a dense layer [81].

2. Sensing

The advantages of using Rydberg atoms to measure electric fields extend to electric field sensing [82]–[84]. Other field parameters, such as phase and polarization, can also be measured using Rydberg atoms. This will greatly expand the application of Rydberg atom sensing and enable Rydberg atom-based electric field sensing.

1) Measurement of microwave electric field phase

Rydberg atoms are further useful in absolute measurements of RF fields using EIT. However, using Rydberg atoms to measure the phase of the RF field remains very challenging. Measuring the phase of RF fields is an essential element of many applications, including antenna metrology, communications, and radar. Holloway, *et al.* demonstrated a scheme for measuring the phase of an RF field [85]–[87] using Rydberg atoms as a mixer to downconvert an RF field of 20 GHz to an intermediate frequency on the order of kHz. The phase of the intermediate frequency corresponded directly to the RF field phase. They used this method to measure the phase shift of electromagnetic waves in horn antennas because the antennas were at different distances from the Rydberg atomic sensor. Atom-based RF phase measurements allow measurement of the propagation constant of RF waves to within 0.1% of theoretical values. Because the phase of an RF field was measurable, Rydberg atom sen-

sors can also be used to measure the angle of arrival (AOA) [88]. When the Rydberg atomic sensor is used to measure the phase at two different locations in the cell, the AOA of the signal can be obtained with a precision of 2.1° using the phase difference.

2) Rydberg atomic microwave frequency comb

Although high measurement sensitivity can be achieved in atomic superheterodyne-based measurement of a microwave electric field, the instantaneous bandwidth is relatively narrow, which critically limits the applications of such a receiver. Thus, new solutions need to be developed to extend the real-time measurement range and realize measurement of a signal with a certain spectral width. To solve related problems, the USTC group proposed using a microwave frequency comb (MFC) to measure a microwave electric field [89]. A microwave was measured precisely using a spectrometer with a Rydberg microwave transition frequency comb modified with multiple microwave fields, in which the modified Rydberg atoms displayed a comb-like RF transition. The Rydberg MFC spectrum provided instantaneous absolute frequency measurement over a range of 125 MHz and the relative phase of single-frequency microwave signals. The method remained valid for microwave signals with a certain spectral width. This experiment facilitated real-time detection of unknown microwave signals over a large spectral range using Rydberg atoms.

3) Large-bandwidth measurement of microwave electric fields

Rydberg atoms respond well to a wide range of microwave electric fields, but continuous measurement of such signals remains quite challenging. To realize continuous large-bandwidth measurement, Paul *et al.* group [90] recently demonstrated an atomic RF receiver and spectrum analyzer based on thermal Rydberg atoms coupled with planar microwave waveguides. Nonresonant RF heterodyne technology was used to achieve continuous operation from DC to the 20 GHz carrier frequency range, as shown in Figure 9. The system is DC-coupled and exhibits inherent sensitivity up to −120(2) dBm/Hz, a 4-MHz instantaneous bandwidth, and a linear dynamic range of over 80 dB.

By using a low-noise preamplifier, high-performance spectral analysis was demonstrated with peak sensitivity better than −145 dBm/Hz. Connecting a standard rabbit ear antenna enabled the spectrum analyzer to detect weak ambient signals, including FM radio, AM radio, WiFi, and Bluetooth. This waveguide coupling greatly strengthened the coupling between free-space microwaves and Rydberg atoms by restricting the electric field to the region of the Rydberg atoms. The system made it possible to develop small, room temperature, integration-based Rydberg sensors that exceeded the typical bandwidth. Such sensors may further exceed the thermal noise limit on the sensitivity of conventional RF sensors, receivers, and analyzers.

4) Vector microwave measurements

Rydberg atomic EIT-AT spectroscopy can also be used to measure microwave polarization [91], [92]. Because the EIT spectrum is sensitive to laser polarization, the microwave polarization angle relative to the laser affects the shape of the spectrum. When the selected atomic energy level is in a four-level system, different results can be obtained by changing the polarization combination of the probe light, coupling light, and microwave electric field, as shown in Figure 10.

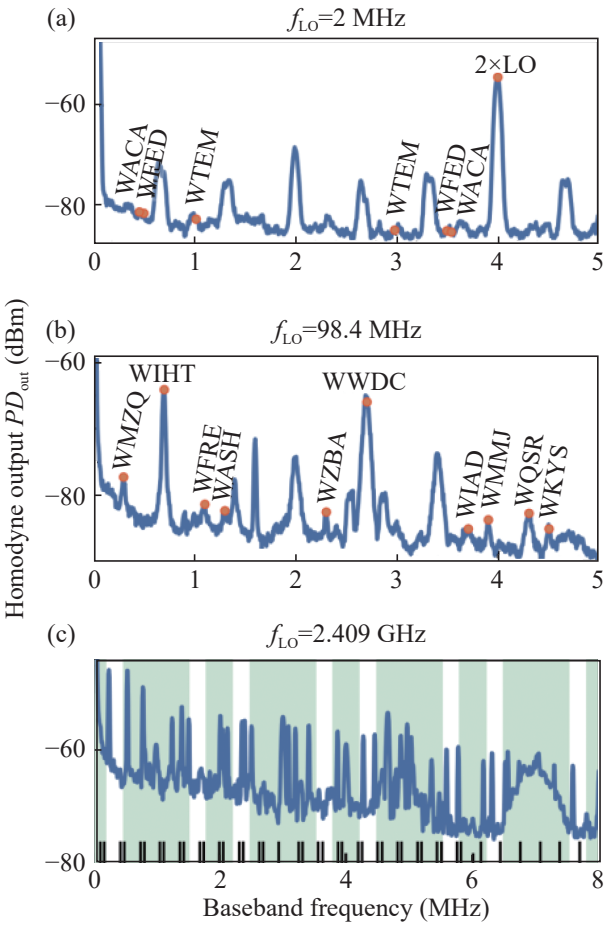

Figure 9 RF signals observed in the laboratory using a rabbit ear antenna. AM radio, FM radio, WLAN, and Bluetooth signals can be observed by tuning the LO to f_{LO} = 2 MHz, 98.4 MHz, and 2.409 GHz [90].

The microwave electric field in different directions can be divided into two parts, one of which couples the Rydberg state and the other of which does not. The relative strength of these two parts depends on the angle between the microwave electric field polarization and the laser polarization, such that changing the microwave polarization direction changes the transmission spectrum of the probe light. When the polarization direction of the probe and the coupled fields is given, the polarization direction of the microwave electric field can be determined, and the polarization angle as measured can be recorded precisely to 0.5°.

V. Outlook

Compared with traditional antenna measurements, electric field measurements based on Rydberg atoms offers unique

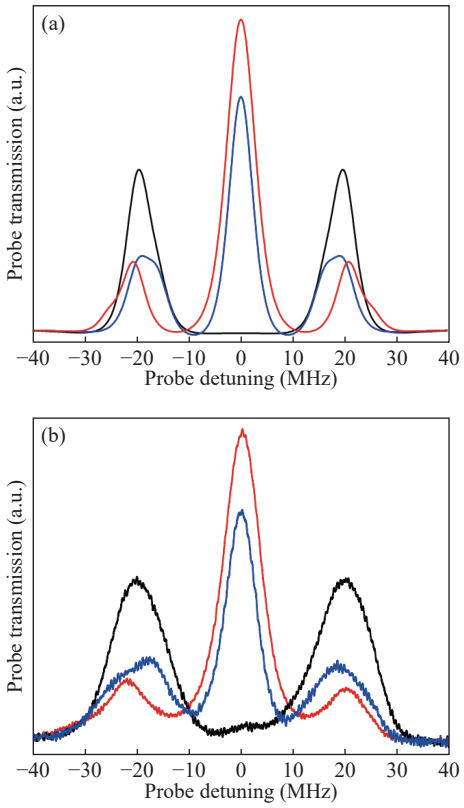

Figure 10 EIT spectrum corresponding to microwaves with different polarization directions [91].

advantages including higher sensitivity, size independence, and large working bandwidth. The interaction between Rydberg atoms and the applied electric field can produce interesting physical outcomes and expand current experimental limits.

Although there has been much progress in enhancing the sensitivity of Rydberg receivers [93], [94], no reports have yet exceeded the sensitivity of conventional microwave receivers. The minimum measurable field strength reached 780 pV/cm [11], and in [95] a best sensitivity of 12.5 nV/(cm·Hz$^{1/2}$) has been reported. The quantum projection noise limit for Rydberg atoms is lower than that of traditional measurement methods, therefore promising higher sensitivity. Further exploration of this effect is of interest [96]. In the future, Rydberg atoms can be used to obtain higher sensitivity and ultimately replace traditional metal antennas in microwave applications.

Continuous operation of Rydberg atomic RF sensing is a fundamental requirement to avoid multiple downconversion events when used as traditional receivers. This paradigm is conducive to directly receiving television, satellite, Wi-Fi, mobile phone, and other signals with a fundamentally different operation than traditional microwave receiving systems. Electric fields have been detected in several separated frequency bands from the kHz to THz regions. However, there exists much room for developing a larger working bandwidth than that of the traditional receiver.

Instantaneous bandwidth is also an important parameter for building a radar based on Rydberg atoms. This parameter determines the resolution of object identification or the communication rate. However, it is limited by the relaxation time over which the atomic system reaches a steady state, which is always in the range of kHz to MHz. Such a relaxation time is far from that of the traditional measurement devices, which often provide an instantaneous bandwidth on the order of GHz. Therefore, new physical effects and technologies need to be exploited to improve this parameter.

In a traditional antenna measurement system, it is necessary to use different antenna sizes to receive different electromagnetic wavelengths. However, Rydberg atomic receivers can be used for continuous broadband signal measurement without changing the sensing element, which is conducive to device miniaturization and integration. This effect would enable the loading of Rydberg sensors on a satellite for sensing MHz electric fields and avoid the traditional use of large MHz radars. Thus, this is very promising for sensing microwave signals in a small aircraft.

Future work can demonstrate the advantages of Rydberg atom sensors with multiple indexes at the same time, such as with indexes for both working bandwidth and sensitivity. The advantages of the Rydberg atom may be specific to special areas such as detecting the field distribution near a signal source, in which the particular requirements of miniaturization and noncalibration could be met perfectly by the Rydberg atoms.

Acknowledgements

This work was supported by the National Key R&D Program of China (Grant No. 2022YFA140400), the National Natural Science Foundation of China (Grant Nos. U20A20 218, 61525504, and 61435011), and the Youth Innovation Promotion Association of the Chinese Academy of Sciences (Grant No. 2018490).

References

[1] J. Kitching, S. Knappe, and E. A. Donley, "Atomic sensors–a review," *IEEE Sensors Journal*, vol. 11, no. 9, pp. 1749–1758, 2011.

[2] J. L. Hall, "Nobel lecture: Defining and measuring optical frequencies," *Reviews of Modern Physics*, vol. 78, no. 4, pp. 1279–1295, 2006.

[3] S. L. Campbell, R. B. Hutson, G. E. Marti, *et al*., "A Fermi-degenerate three-dimensional optical lattice clock," *Science*, vol. 358, no. 6359, pp. 90–94, 2017.

[4] W. F. McGrew, X. Zhang, R. J. Fasano, *et al*., "Atomic clock performance enabling geodesy below the centimetre level," *Nature*, vol. 564, no. 7734, pp. 87–90, 2018.

[5] Q. Shen, J. Y. Guan, J. G. Ren, *et al*., "Free-space dissemination of time and frequency with 10^{-19} instability over 113 km," *Nature*, vol. 610, no. 7933, pp. 661–666, 2022.

[6] M. V. Balabas, T. Karaulanov, M. P. Ledbetter, *et al*., "Polarized alkali-metal vapor with minute-long transverse spin-relaxation time," *Physical Review Letters*, vol. 105, no. 7, article no. 070801, 2010.

[7] M. Koschorreck, M. Napolitano, B. Dubost, *et al*., "Quantum nondemolition measurement of large-spin ensembles by dynamical decoupling," *Physical Review Letters*, vol. 105, no. 9, article no.

093602, 2010.

[8] I. M. Savukov, S. J. Seltzer, M. V. Romalis, *et al*., "Tunable atomic magnetometer for detection of radio-frequency magnetic fields," *Physical Review Letters*, vol. 95, no. 6, article no. 063004, 2005.

[9] W. Wasilewski, K. Jensen, H. Krauter, *et al*., "Quantum noise limited and entanglement-assisted magnetometry," *Physical Review Letters*, vol. 104, no. 13, article no. 133601, 2010.

[10] A. Facon, E. K. Dietsche, D. Grosso, *et al*., "A sensitive electrometer based on a Rydberg atom in a schrdinger-cat state," *Nature*, vol. 535, no. 7611, pp. 262–265, 2016.

[11] M. Y. Jing, Y. Hu, J. Ma, *et al*., "Atomic superheterodyne receiver based on microwave-dressed Rydberg spectroscopy," *Nature Physics*, vol. 16, no. 9, pp. 911–915, 2020.

[12] J. A. Sedlacek, A. Schwettmann, H. Kübler, *et al*., "Microwave electrometry with Rydberg atoms in a vapour cell using bright atomic resonances," *Nature Physics*, vol. 8, no. 11, pp. 819–824, 2012.

[13] M. Fleischhauer, A. Imamoglu, and J. P. Marangos, "Electromagnetically induced transparency: Optics in coherent media," *Reviews of Modern Physics*, vol. 77, no. 2, pp. 633–673, 2005.

[14] H. Kübler, J. P. Shaffer, T. Baluktsian, *et al*., "Coherent excitation of Rydberg atoms in micrometre-sized atomic vapour cells," *Nature Photonics*, vol. 4, no. 2, pp. 112–116, 2010.

[15] A. K. Mohapatra, T. R. Jackson, and C. S. Adams, "Coherent optical detection of highly excited Rydberg states using electromagnetically induced transparency," *Physical Review Letters*, vol. 98, no. 11, article no. 113003, 2007.

[16] H. M. Kwak, T. Jeong, Y. S. Lee, *et al*., "Microwave-induced three-photon coherence of Rydberg atomic states," *Optics Communications*, vol. 380, pp. 168–173, 2016.

[17] M. Tanasittikosol, J. D. Pritchard, D. Maxwell, *et al*., "Microwave dressing of Rydberg dark states," *Journal of Physics B: Atomic, Molecular and Optical Physics*, vol. 44, no. 18, article no. 184020, 2011.

[18] T. F. Gallagher, "Rydberg atoms," *Reports on Progress in Physics*, vol. 51, no. 2, pp. 143–188, 1988.

[19] S. E. Harris and L. V. Hau, "Nonlinear optics at low light levels," *Physical Review Letters*, vol. 82, no. 23, pp. 4611–4614, 1999.

[20] N. B. Delone and V. P. Krainov, "AC stark shift of atomic energy levels," *Physics-Uspekhi*, vol. 42, no. 7, pp. 669–687, 1999.

[21] J. S. Bakos, "AC stark effect and multiphoton processes in atoms," *Physics Reports*, vol. 31, no. 3, pp. 209–235, 1977.

[22] S. K. Son, S. Y. Han, and S. I. Chu, "Floquet formulation for the investigation of multiphoton quantum interference in a superconducting qubit driven by a strong ac field," *Physical Review A*, vol. 79, no. 3, article no. 032301, 2009.

[23] S. Yoshida, C. O. Reinhold, J. Burgdrfer, *et al*., "Photoexcitation of $n\simeq305$ Rydberg states in the presence of an rf drive field," *Physical Review A*, vol. 86, no. 4, article no. 043415, 2012.

[24] J. H. Shirley, "Solution of the schrdinger equation with a Hamiltonian periodic in time," *Physical Review*, vol. 138, no. 4B, pp. B979–B987, 1965.

[25] J. D. Carter, O. Cherry, and J. D. D. Martin, "Electric-field sensing near the surface microstructure of an atom chip using cold Rydberg atoms," *Physical Review A*, vol. 86, no. 5, article no. 053401, 2012.

[26] F. Osterwalder and A. Merkt, "Using high Rydberg states as electric field sensors," *Physical Review Letters*, vol. 82, no. 9, pp. 1831–1834, 1999.

[27] L. A. Jones, J. D. Carter, and J. D. D. Martin, "Rydberg atoms with a reduced sensitivity to dc and low-frequency electric fields," *Physical Review A*, vol. 87, no. 2, article no. 023423, 2013.

[28] R. P. Abel, C. Carr, U. Krohn, *et al*., "Electrometry near a dielectric surface using Rydberg electromagnetically induced transparency," *Physical Review A*, vol. 84, no. 2, article no. 023408, 2011.

[29] M. G. Bason, M. Tanasittikosol, A. Sargsyan, *et al*., "Enhanced electric field sensitivity of rf-dressed Rydberg dark states," *New Journal of Physics*, vol. 12, no. 6, article no. 065015, 2010.

[30] A. K. Mohapatra, M. G. Bason, B. Butscher, *et al*., "A giant electro-optic effect using polarizable dark states," *Nature Physics*, vol. 4, no. 11, pp. 890–894, 2008.

[31] M. Viteau, J. Radogostowicz, M. G. Bason, *et al*., "Rydberg spectroscopy of a Rb MOT in the presence of applied or ion created electric fields," *Optics Express*, vol. 19, no. 7, pp. 6007–6019, 2011.

[32] H. Q. Fan, S. Kumar, J. Sedlacek, *et al*., "Atom based RF electric field sensing," *Journal of Physics B: Atomic, Molecular and Optical Physics*, vol. 48, no. 20, article no. 202001, 2015.

[33] C. L. Holloway, M. T. Simons, J. A. Gordon, *et al*., "Electric field metrology for SI traceability: Systematic measurement uncertainties in electromagnetically induced transparency in atomic vapor," *Journal of Applied Physics*, vol. 121, no. 23, article no. 233106, 2017.

[34] D. H. Meyer, Z. A. Castillo, K. C. Cox, *et al*., "Assessment of Rydberg atoms for wideband electric field sensing," *Journal of Physics B: Atomic, Molecular and Optical Physics*, vol. 53, no. 3, article no. 034001, 2020.

[35] C. G. Wade, M. Marcuzzi, E. Levi, *et al*., "A terahertz-driven non-equilibrium phase transition in a room temperature atomic vapour," *Nature Communications*, vol. 9, no. 1, article no. 3567, 2018.

[36] Y. Y. Jau and T. Carter, "Vapor-cell-based atomic electrometry for detection frequencies below 1 kHz," *Physical Review Applied*, vol. 13, no. 5, article no. 054034, 2020.

[37] D. A. Anderson and G. Raithel, "Continuous-frequency measurements of high-intensity microwave electric fields with atomic vapor cells," *Applied Physics Letters*, vol. 111, no. 5, article no. 053504, 2017.

[38] D. A. Anderson, A. Schwarzkopf, S. A. Miller, *et al*., "Two-photon microwave transitions and strong-field effects in a room-temperature Rydberg-atom gas," *Physical Review A*, vol. 90, no. 4, article no. 043419, 2014.

[39] S. Coop, S. Palacios, P. Gomez, *et al*., "Floquet theory for atomic light-shift engineering with near-resonant polychromatic fields," *Optics Express*, vol. 25, no. 26, pp. 32550–32559, 2017.

[40] C. Veit, G. Epple, H. Kübler, *et al*., "RF-dressed Rydberg atoms in hollow-core fibres," *Journal of Physics B: Atomic, Molecular and Optical Physics*, vol. 49, no. 13, article no. 134005, 2016.

[41] Y. C. Jiao, X. X. Han, Z. W. Yang, *et al*., "Spectroscopy of cesium Rydberg atoms in strong radio-frequency fields," *Physical Review A*, vol. 94, no. 2, article no. 023832, 2016.

[42] S. A. Miller, D. A. Anderson, and G. Raithel, "Radio-frequency-modulated Rydberg states in a vapor cell," *New Journal of Physics*, vol. 18, no. 5, article no. 053017, 2016.

[43] D. A. Anderson, S. A. Miller, G. Raithel, *et al*., "Optical measurements of strong microwave fields with Rydberg atoms in a vapor cell," *Physical Review Applied*, vol. 5, no. 3, article no. 034003, 2016.

[44] E. Paradis, G. Raithel, and D. A. Anderson, "Atomic measurements of high-intensity vhf-band radio-frequency fields with a Rydberg vapor-cell detector," *Physical Review A*, vol. 100, no. 1, article no. 013420, 2019.

[45] B. Liu, L. H. Zhang, Z. K. Liu, *et al*., "Highly sensitive measurement of a megahertz rf electric field with a Rydberg-atom sensor," *Physical Review Applied*, vol. 18, no. 1, article no. 014045, 2022.

[46] H. Kübler, J. Keaveney, C. Lui, *et al*., "Atom-based sensing of microwave electric fields using highly excited atoms: Mechanisms affecting sensitivity," in *Proceedings of SPIE 10934, Optical, Opto-Atomic, and Entanglement-Enhanced Precision Metrology*, San

Francisco, CA, USA, article no.1093406, 2019.

[47] S. Kumar, H. Q. Fan, H. Kübler, *et al*., "Rydberg-atom based radio-frequency electrometry using frequency modulation spectroscopy in room temperature vapor cells," *Optics Express*, vol. 25, no. 8, pp. 8625–8637, 2017.

[48] M. T. Simons, J. A. Gordon, C. L. Holloway, *et al*., "Using frequency detuning to improve the sensitivity of electric field measurements via electromagnetically induced transparency and Autler-Townes splitting in Rydberg atoms," *Applied Physics Letters*, vol. 108, no. 17, article no. 174101, 2016.

[49] S. Kumar, H. Q. Fan, H. Kübler, *et al*., "Atom-based sensing of weak radio frequency electric fields using homodyne readout," *Scientific Reports*, vol. 7, no. 1, article no. 42981, 2017.

[50] D. S. Ding, Z. K. Liu, B. S. Shi, *et al*., "Enhanced metrology at the critical point of a many-body Rydberg atomic system," *Nature Physics*, vol. 18, no. 12, pp. 1447–1452, 2022.

[51] P. Zanardi, M. G. A. Paris, and L. Campos Venuti, "Quantum criticality as a resource for quantum estimation," *Physical Review A*, vol. 78, no. 4, article no. 042105, 2008.

[52] K. Macieszczak, M. Guţă, I. Lesanovsky, *et al*., "Dynamical phase transitions as a resource for quantum enhanced metrology," *Physical Review A*, vol. 93, no. 2, article no. 022103, 2016.

[53] V. Montenegro, U. Mishra, and A. Bayat, "Global sensing and its impact for quantum many-body probes with criticality," *Physical Review Letters*, vol. 126, no. 20, article no. 200501, 2021.

[54] C. Carr, R. Ritter, C. G. Wade, *et al*., "Nonequilibrium phase transition in a dilute Rydberg ensemble," *Physical Review Letters*, vol. 111, no. 11, article no. 113901, 2013.

[55] D. S. Ding, H. Busche, B. S. Shi, *et al*., "Phase diagram and self-organizing dynamics in a thermal ensemble of strongly interacting Rydberg atoms," *Physical Review X*, vol. 10, no. 2, article no. 021023, 2020.

[56] M. Kiffner, A. Feizpour, K. T. Kaczmarek, *et al*., "Two-way interconversion of millimeter-wave and optical fields in Rydberg gases," *New Journal of Physics*, vol. 18, no. 9, article no. 093030, 2016.

[57] J. P. Covey, A. Sipahigil, and M. Saffman, "Microwave-to-optical conversion via four-wave mixing in a cold ytterbium ensemble," *Physical Review A*, vol. 100, no. 1, article no. 012307, 2019.

[58] J. S. Han, T. Vogt, C. Gross, *et al*., "Coherent microwave-to-optical conversion via six-wave mixing in Rydberg atoms," *Physical Review Letters*, vol. 120, no. 9, article no. 093201, 2018.

[59] T. Vogt, C. Gross, J. S. Han, *et al*., "Efficient microwave-to-optical conversion using Rydberg atoms," *Physical Review A*, vol. 99, no. 2, article no. 023832, 2019.

[60] H. T. Tu, K. Y. Liao, Z. X. Zhang, *et al*., "High-efficiency coherent microwave-to-optics conversion via off-resonant scattering," *Nature Photonics*, vol. 16, no. 4, pp. 291–296, 2022.

[61] C. Jansen, S. Wietzke, O. Peters, *et al*., "Terahertz imaging: Applications and perspectives," *Applied Optics*, vol. 49, no. 19, pp. E48–E57, 2010.

[62] P. U. Jepsen, D. G. Cooke, and M. Koch, "Terahertz spectroscopy and imaging-Modern techniques and applications," *Laser & Photonics Reviews*, vol. 5, no. 1, pp. 124–166, 2011.

[63] L. A. Downes, A. R. MacKellar, D. J. Whiting, *et al*., "Full-field terahertz imaging at kilohertz frame rates using atomic vapor," *Physical Review X*, vol. 10, no. 1, article no. 011027, 2020.

[64] J. A. Gordon, C. L. Holloway, A. Schwarzkopf, *et al*., "Millimeter wave detection via Autler-Townes splitting in rubidium Rydberg atoms," *Applied Physics Letters*, vol. 105, no. 2, article no. 024104, 2014.

[65] D. A. Anderson, R. E. Sapiro, and G. Raithel, "A self-calibrated SI-traceable Rydberg atom-based radio frequency electric field probe and measurement instrument," *IEEE Transactions on Antennas and Propagation*, vol. 69, no. 9, pp. 5931–5941, 2021.

[66] A. Artusio-Glimpse, M. T. Simons, N. Prajapati, *et al*., "Modern RF measurements with hot atoms: A technology review of Rydberg atom-based radio frequency field sensors," *IEEE Microwave Magazine*, vol. 23, no. 5, pp. 44–56, 2022.

[67] M. T. Simons, A. H. Haddab, J. A. Gordon, *et al*., "Embedding a Rydberg atom-based sensor into an antenna for phase and amplitude detection of radio-frequency fields and modulated signals," *IEEE Access*, vol. 7, pp. 164975–164985, 2019.

[68] C. L. Holloway, M. T. Simons, J. A. Gordon, *et al*., "Atom-based RF electric field metrology: From self-calibrated measurements to subwavelength and near-field imaging," *IEEE Transactions on Electromagnetic Compatibility*, vol. 59, no. 2, pp. 717–728, 2017.

[69] C. T. Fancher, D. R. Scherer, M. C. St. John, *et al*., "Rydberg atom electric field sensors for communications and sensing," *IEEE Transactions on Quantum Engineering*, vol. 2, article no. 3501313, 2021.

[70] D. A. Anderson, R. E. Sapiro, and G. Raithel, "Rydberg atoms for radio-frequency communications and sensing: Atomic receivers for pulsed RF field and phase detection," *IEEE Aerospace and Electronic Systems Magazine*, vol. 35, no. 4, pp. 48–56, 2020.

[71] A. B. Deb and N. Kjærgaard, "Radio-over-fiber using an optical antenna based on Rydberg states of atoms," *Applied Physics Letters*, vol. 112, no. 21, article no. 211106, 2018.

[72] C. Holloway, M. Simons, A. H. Haddab, *et al*., "A multiple-band Rydberg atom-based receiver: AM/FM stereo reception," *IEEE Antennas and Propagation Magazine*, vol. 63, no. 3, pp. 63–76, 2021.

[73] D. A. Anderson, R. E. Sapiro, and G. Raithel, "An atomic receiver for AM and FM radio communication," *IEEE Transactions on Antennas and Propagation*, vol. 69, no. 5, pp. 2455–2462, 2021.

[74] Y. C. Jiao, X. X. Han, J. B. Fan, *et al*., "Atom-based receiver for amplitude-modulated baseband signals in high-frequency radio communication," *Applied Physics Express*, vol. 12, no. 12, article no. 126002, 2019.

[75] S. M. Bohaichuk, D. Booth, K. Nickerson, *et al*., "Origins of Rydberg-atom electrometer transient response and its impact on radio-frequency pulse sensing," *Physical Review Applied*, vol. 18, no. 3, article no. 034030, 2022.

[76] C. L. Holloway, M. T. Simons, A. H. Haddab, *et al*., "A "real-time" guitar recording using Rydberg atoms and electromagnetically induced transparency: Quantum physics meets music," *AIP Advances*, vol. 9, no. 6, article no. 065110, 2019.

[77] C. L. Holloway, M. T. Simons, J. A. Gordon, *et al*., "Detecting and receiving phase-modulated signals with a Rydberg atom-based receiver," *IEEE Antennas and Wireless Propagation Letters*, vol. 18, no. 9, pp. 1853–1857, 2019.

[78] D. H. Meyer, K. C. Cox, F. K. Fatemi, *et al*., "Digital communication with Rydberg atoms and amplitude-modulated microwave fields," *Applied Physics Letters*, vol. 112, no. 21, article no. 211108, 2018.

[79] K. C. Cox, D. H. Meyer, F. K. Fatemi, *et al*., "Quantum-limited atomic receiver in the electrically small regime," *Physical Review Letters*, vol. 121, no. 11, article no. 110502, 2018.

[80] Z. F. Song, H. P. Liu, X. C. Liu, *et al*., "Rydberg-atom-based digital communication using a continuously tunable radio-frequency carrier," *Optics Express*, vol. 27, no. 6, pp. 8848–8857, 2019.

[81] Z. K. Liu, L. H. Zhang, B. Liu, *et al*., "Deep learning enhanced Rydberg multifrequency microwave recognition," *Nature Communications*, vol. 13, no. 1, article no. 1997, 2022.

[82] D. T. Stack, P. D. Kunz, D. H. Meyer, *et al*., "Microwave electric field sensing with Rydberg atoms," in *Proceedings of SPIE 9873, Quantum Information and Computation IX*, Baltimore, MD, USA, article no.987306, 2016.

[83] C. L. Holloway, J. A. Gordon, S. Jefferts, *et al*., "Broadband Rydberg atom-based electric-field probe for SI-traceable, self-calibrated measurements," *IEEE Transactions on Antennas and Propagation*, vol. 62, no. 12, pp. 6169–6182, 2014.

[84] C. L. Holloway, J. A. Gordon, A. Schwarzkopf, *et al*., "Sub-wavelength imaging and field mapping via electromagnetically induced transparency and Autler-Townes splitting in Rydberg atoms," *Applied Physics Letters*, vol. 104, no. 24, article no. 244102, 2014.

[85] M. T. Simons, A. H. Haddab, J. A. Gordon, *et al*., "A Rydberg atom-based mixer: Measuring the phase of a radio frequency wave," *Applied Physics Letters*, vol. 114, no. 11, article no. 114101, 2019.

[86] J. A. Gordon, M. T. Simons, A. H. Haddab, *et al*., "Weak electric-field detection with sub-1 Hz resolution at radio frequencies using a Rydberg atom-based mixer," *AIP Advances*, vol. 9, no. 4, article no. 045030, 2019.

[87] S. Berweger, A. B. Artusio-Glimpse, A. P. Rotunno, *et al*., "Phase-resolved Rydberg atom field sensing using quantum interferometry," *arXiv preprint*, arXiv: 2212.00185, 2022.

[88] A. K. Robinson, N. Prajapati, D. Senic, *et al*., "Determining the angle-of-arrival of a radio-frequency source with a Rydberg atom-based sensor," *Applied Physics Letters*, vol. 118, no. 11, article no. 114001, 2021.

[89] L. H. Zhang, Z. K. Liu, B. Liu, *et al*., "Rydberg microwave-frequency-comb spectrometer," *Physical Review Applied*, vol. 18, no. 1, article no. 014033, 2022.

[90] D. H. Meyer, P. D. Kunz, and K. C. Cox, "Waveguide-coupled Rydberg spectrum analyzer from 0 to 20 GHz," *Physical Review Applied*, vol. 15, no. 1, article no. 014053, 2021.

[91] J. A. Sedlacek, A. Schwettmann, H. Kübler, *et al*., "Atom-based vector microwave electrometry using rubidium Rydberg atoms in a vapor cell," *Physical Review Letters*, vol. 111, no. 6, article no. 063001, 2013.

[92] Y. C. Jiao, L. P. Hao, X. X. Han, *et al*., "Atom-based radio-frequency field calibration and polarization measurement using cesium nD_J floquet states," *Physical Review Applied*, vol. 8, no. 1, article no. 014028, 2017.

[93] C. L. Holloway, N. Prajapati, A. B. Artusio-Glimpse, *et al*., "Rydberg atom-based field sensing enhancement using a split-ring resonator," *Applied Physics Letters*, vol. 120, no. 20, article no. 204001, 2022.

[94] N. Prajapati, A. K. Robinson, S. Berweger, *et al*., "Enhancement of electromagnetically induced transparency based Rydberg-atom electrometry through population repumping," *Applied Physics Letters*, vol. 119, no. 21, article no. 214001, 2021.

[95] M. H. Cai, Z. S. Xu, S. H. You, *et al*., "Sensitivity improvement and determination of Rydberg atom-based microwave sensor," *Photonics*, vol. 9, no. 4, article no. 250, 2022.

[96] G. Santamaria-Botello, S. Verploegh, E. Bottomley, *et al*., "Comparison of noise temperature of Rydberg-atom and electronic microwave receivers," *arXiv preprint*, arXiv: 2209.00908, 2022.

Bang Liu received the B.S. degree in optical engineering from the University of Science and Technology of China, Hefei, China, in 2020. He is now a Ph.D. candidate in physics in the Synergetic Innovation Center of Quantum Information and Quantum Physics, Hefei, China. His research interests include quantum precision measurements based on Rydberg atoms, atomic electric field sensing, quantum simulation and quantum computing based on neutral atomic systems.
(Email: lb2016wu@mail.ustc.edu.cn)

Lihua Zhang received the B.S. degree in physics from Shanxi University, Taiyuan, China, in 2019. He is now a Ph.D. candidate in physics in the Key Laboratory of Quantum Information, Hefei, China. His research interests include quantum precision measurements based on Rydberg atoms, atomic electric field sensing, quantum simulation and quantum computing based on neutral atomic systems. (Email: zlhphys@mail.ustc.edu.cn)

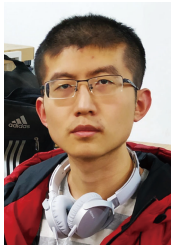

Zongkai Liu received the B.S. degree in physics from Taiyuan University of Technology, Taiyuan, China, in 2019. He is now a Ph.D. candidate in physics in the Synergetic Innovation Center of Quantum Information and Quantum Physics, Hefei, China. His research interests include quantum precision measurements based on Rydberg atoms, atomic electric field sensing, quantum simulation and quantum computing based on neutral atomic systems. He is also interested in machine learning and artificial intelligence. (Email: lzk1997@mail.ustc.edu.cn)

Zian Deng is studying for the B.S. degree in the Department of Physics at the University of Science and Technology of China. His research interests include quantum precision measurements based on Rydberg atoms, atomic electric field sensing, quantum simulation and quantum computing based on neutral atomic systems.
(Email: dza@mail.ustc.edu.cn)

Dongsheng Ding received the Ph.D. degree in physics from the University of Science and Technology of China in 2015. From 2015 to 2018, he was an Assistant Researcher at the Department of Physics, University of Science and Technology of China. From 2018 to now, he has been a Professor at the University of Science and Technology of China. He is mainly engaged in quantum storage and quantum communication based on cold atomic ensembles, quantum computing and quantum simulation based on Rydberg atoms and quantum sensing based on Rydberg atoms.

Dr. Ding is the recipient of the special award of the Chinese Academy of Sciences in 2015, and the Outstanding Doctoral Dissertation Award of the Chinese Academy of Sciences in 2016. He was invited to write a monograph on Springer Theses, which is the best doctoral thesis from top international research institutions. He has published more than 90 SCI papers in recent years. His innovative results have been selected for Research Highlights and News&Views in *MIT Technology Review*, *Physics Org*, *Physics ViewPoint*, *Pro-physik.de*, *Nature Photonics*, and *Nature Physics*.
(Email: dds@ustc.edu.cn)

Baosen Shi received the Ph.D. degree from the Department of Physics, University of Science and Technology of China in 1998, under the supervision of Academician Guangcan Guo. He stayed in the university to teach and was responsible for the establishment of the Laboratory of Nonlinear Optics under the support of the "211" Project and the establishment of the Laboratory of Quantum Information on this basis. From April 2001 to November 2004, he was a Researcher of the Japan Science and Technology Agency (JSTA) and conducted theoretical and experimental

research on quantum optics, nonlinear optics and quantum information at the NEC Institute of Fundamental Research in Japan. He was selected by the Ministry of Education as one of the "New Century Excellent Talent Support Program" in 2007 and was awarded the National Outstanding Youth Fund by the Natural Science Foundation of China in 2015. He is mainly engaged in theoretical and experimental research on quantum information, nonlinear optics, integrated optics and quantum optics and has published more than 100 papers as first/corresponding author in famous academic journals in *Sci. Adv.*, *Nat. Photo.*, *Nat. Comm.*, *PRL*, *PRX*, etc. (Email: drshi@ustc.edu.cn)

Guangcan Guo graduated from the Department of Radio Electronics of the University of Science and Technology of China in July 1965 and was elected as Academician of Chinese Academy of Sciences in 2003 and the Academy of Sciences for the Developing World in 2009. He was the Director of the Key Laboratory of Quantum Information of the Chinese Academy of Sciences, the Executive Director of the Chinese Physical Society, the President of the Optical Society of China, the Director of the Academic Committee of the Collaborative Innovation Center of Quantum Information and Quantum Science and Technology Frontier of the Ministry of Education (2011 Program), and the Director of the Solid State Quantum Information Research Department. He was also the Chief Scientist of the 973 Project "Quantum Communication and Quantum Information Technology" of the Ministry of Science and Technology of the People's Republic of China and the Chief Scientist of the Strategic Pioneering Science and Technology Project of the Chinese Academy of Sciences. He was also the Chief Scientist of the "Quantum Physics and Quantum Information in Solid State Systems" project of the Chinese Academy of Sciences and the Academic Leader of the Innovation Group of the National Foundation of China. He was the Chief Scientist of the "Quantum Regulation" project of the Ministry of Science and Technology of China and the Chief Scientist of the "Physical Implementation of Quantum Communication and Quantum Computing" project. He was selected as an advanced worker of the Chinese Academy of Sciences and a national outstanding teacher of the Ministry of Education. He is mainly engaged in theoretical and experimental research on quantum optics, quantum cryptography, quantum communication and quantum computing. He has published more than 700 SCI papers, including Nature subpublications and PRL papers, with more than 10,000 SCI citations. He has published 7 monographs. (Email: gcguo@ustc.edu.cn)